IUST
Iran University of Science and Technology

Iranian Journal of Electrical and Electronic Engineering

Journal Homepage: ijeee.iust.ac.ir

Research Paper

A Study on Switching Intervals in Classic DTC for Induction Motor

A. Ghayebloo*(C.A.) and S. Shiri*

Abstract: In this paper, a conceptual study on switching intervals in the classic direct torque control (DTC) method and a novel modified method have been proposed. In the switching table of classic DTC, the switching vectors have been changed in sectors with 60 degrees intervals and their boundaries are fixed. In this study, these fixed boundaries and length of switching intervals have been challenged and proved that the performance of the classic DTC can be improved with modified intervals with different lengths and boundaries. The final proposed switching table not also benefits simplicity of implementation as classic DTC switching table, but also it offers better performance especially in the aspect of low torque ripples. The proposed final switching table has been derived by a two-stage optimization process and the results have been proved by simulation results.

Keywords: Classic DTC, Switching Intervals, Optimality Aspects, Induction Motor.

1 Introduction

ACCORDING to the statistical reports related to energy consumption, fifty percent of produced electric energy consumes by electric machines [1]. Because of structural reasons, in DC motors decoupled control of speed and torque can be achieved. Compared to DC motors, induction motors have complicated and nonlinear mathematical model cause that the decoupled speed and torque control be complicated [2]. But induction motors have important benefits such as simple structure, low cost and high reliability therefore a lot of researches have been developed in recent decades about them.

In a global view, the control methods of AC machines categorized into two groups named scalar and vector control methods [2]. The scalar methods such as constant v/f utilize the steady-state model of machine while the vector control methods are based on machine dynamic model and can control the angular position of space vectors in addition to their amplitudes. This ability causes enhanced speed response and control performance in steady-state and transient conditions [3].

Field Oriented Control (FOC) and Direct Torque Control (DTC) are two well-known advanced electrical machines control methods. Compared to FOC, DTC has a simple structure and acceptable fast dynamic response [4]. In this approach, mathematical burdens related to current controllers and coordinate transformations there not exist but it has high flux and torque ripples cause to some problems especially in very low speed range. The mentioned disadvantages lead to various suggestions to improve performance of this method such as Predictive Torque Control (PTC) [5], Space Vector Modulation Direct Torque Control (SVM-DTC) [6], DTC with duty cycle control [7], and DTC with single current sensor [8, 9]. Most of these new approaches have high computational volume and they eliminate the main advantage of DTC i.e. its simplicity.

The main idea of this study is to investigate of DTC concept with numerical simulations to improve its performance, especially in flux and torque ripple reduction view without missing its simplicity. In most of the previous works such as [12-16] predictive approach has been applied to minimize the torque and flux ripples. As mentioned, this approach has high computational volume and eliminates the simplicity advantage of DTC method. The important contribution of this paper is proposing four conceptual challenging questions to classic DTC approach. These four questions about the classic DTC have been asked and tried to answer as below.

Iranian Journal of Electrical and Electronic Engineering, 2021.
Paper first received 12 April 2020, revised 19 February 2021, and accepted 06 March 2021.
* The authors are with the Engineering Department, University of Zanjan, Zanjan, Iran.
E-mails: a.ghayebloo@znu.ac.ir and saeid.shiri@znu.ac.ir.
Corresponding Author: A. Ghayebloo.
https://doi.org/10.22068/IJEEE.17.4.1856

1. Why the switching intervals length is 60°?
2. Are the boundaries of the switching intervals must be 30°, 90°, etc., and cannot be changed to improve performance?
3. Is the classic DTC switching table optimal for all operation points or it is optimal for only nominal point?
4. What is the optimality of the classic DTC switching table? Fast dynamic, reduced flux or torque ripple, efficiency, or other?

In this paper, all these challenges being studied by simulations. It is proofed that the assumptions of classic DTC, such as fixed 60° switching intervals length, their fixed boundaries, and the optimality criterions all can be disturbed and changed to improve this method drawbacks such as its high torque and flux ripples. It must be noted that this improvement can be achieved by no more computational efforts and the simplicity of this method remains unchanged.

In this paper, a novel switching table for DTC has been proposed. This table has different sections, boundaries, and suggested vectors compared with the switching table of classic DTC but it has its simplicity. The proposed switching table has been derived with off-line examining the torque and flux ripples in a proper cost function in various operating points and with various weighting factors. In off-line simulations, at the first stage, in any sample time, the normalized difference of torque and difference of flux amplitude per all switching vectors are calculated and according to a cost function, similar to conventional predictive torque control (PTC), the best switching vector will be selected. The next stage of the proposed approach is optimizing the weighting factor of the selected cost function by multiple simulations. In the final stage of the proposed approach, the selected fitness function and its optimum weighting factor are simulated in multiple operating points to extract the final switching table with averaged boundaries.

The remainder of the paper is organized as follows. In Section 2 induction machine model and classic DTC method are briefly discussed. Section 3 describes the proposed methodology in detail and Section 4 represents the results of the study. Finally, some conclusions are provided in Section 5.

2 Motor Model and Classic DTC

The induction machine dynamic model can be expressed by (1) in an arbitrary reference frame rotating with speed ω [10]. These equations will be used in Section 3 for extracting the equations of the proposed method.

$$
\begin{aligned}
&V_{dqos} = r_s i_{dqos} + \omega\lambda_{qds} + p\lambda_{dqos}\\
&V'_{dqor} = r'_r i'_{dqor} + (\omega - \omega_r)\lambda'_{qdr} + p\lambda'_{dqor}\\
&\lambda_{dqos} = L_{ls} i_{dqos} + L_M\left(i_{dqos} + i'_{dqor}\right)\\
&\lambda'_{dqor} = L'_{lr} i'_{dqor} + L_M\left(i_{dqos} + i'_{dqor}\right)\\
&T_e = \frac{3}{2}P\left(i_{ds}\lambda_{qs} - i_{qs}\lambda_{ds}\right)\\
&T_e - T_L = Jp\omega_r + B\omega_r\\
&\left(\lambda_{qdx}\right)^T = \left[\lambda_{qx} \;\; -\lambda_{dx} \;\; 0\right], x = s, r\\
&\left(X_{dqo}\right)^T = \left[X_d \;\; X_q \;\; X_o\right], x = v, i, \lambda
\end{aligned}
\tag{1}
$$

where P is the machine pole pairs, p is the derivation operator, ω_r is the rotor electrical rotational speed, L_{lx} and L_M are the leakage and mutual inductances, λ refers to the machine flux and r_s and r'_r are the stator and referred rotor resistances respectively. In this equation, d, q, o, s, and r lower indices are related to direct axis, quadrature axis, zero term, stator and rotor, respectively. Also, T_e, T_L, J, and B are electromagnetic torque, load torque, moment of inertia and bearing coefficient, respectively. It is known that in DTC method for eliminating the calculation burden related to frame transformations, the stationary reference frame with $\omega = 0$ is used.

At first, DTC has been presented based on Takahashi Isao studies [4] in the middle of 80 decade. The block diagram of the classic DTC is depicted in Fig. 1. As shown in this figure, the amplitude of machine torque and flux, after estimation, have been controlled by means of two independent hysteresis controllers via a switching table.

The key part of the DTC method is its switching table. The inputs of this table are the digital output states of two hysteresis controllers and the output is the number of switching vector of traditional VSI inverter which has 6 active and two zero vectors. Fig. 2 shows the switching vectors and sectors in the space vectors plane.

In the classic DTC method, for deriving the switching table a simple idea is used. It can be derived from torque and flux estimation equations with some assumptions written in stationary reference frame, that the amplitude of the machine torque can be changed rapidly if the rotational angle of the stator flux has been changed as rapidly as possible. This can be performed by selecting the semi-orthogonal voltage vector with respect to the current position of the stator flux vector. Also, the amplitude of the machine flux can be changed rapidly if the more aligned voltage vector with respect to the current position of the stator flux vector has been selected. According to this idea, in the global view, if the stator flux be in sector n, applying the vectors V_{n-1}, V_n, V_{n+1} leads to increased flux amplitude and applying the vectors V_{n-2}, V_{n+2}, V_{n+3} leads to decreased flux amplitude. On the other hand, vectors V_{n+1} and V_{n+2} cause to increase in machine torque, and applying the V_{n-1} and V_{n-2} vectors cause in decreasing it. The vectors V_n and V_{n+3} depending to flux position can increase of decrease the produced torque. Table 1 shows these statements briefly.

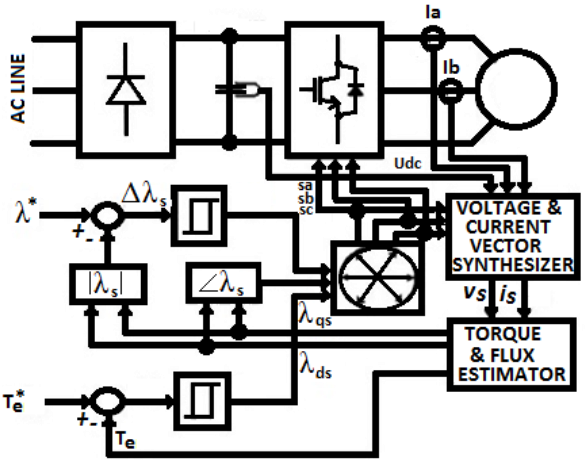

Fig. 1 The classic DTC block diagram [11].

3 The Proposed Approach

As mentioned in section 1, some basic questions could be proposed about the classic DTC methodology. In this section, the approach of this study to reply to these questions will be described. In this approach at first, in any sampling time of the control, the difference of torque and flux amplitudes per all switching vectors are calculated and according to a fitness function, the best switching vector will be selected.

The first stage of the proposed approach is similar to the conventional predictive torque control (PTC) with one prediction and control horizon. Predictive control is an effective approach especially for systems which have limited choices for the control signal. In these systems, the control command can be selected only within a discrete set. The control of electric machines with inverters has this feature. It is well-known that in conventional two-level voltage source inverters (VSIs), only six active and two zero voltage vectors can be applied to the machine. In the PTC method, in any control intervals, the desired cost function is calculated to all possible control set and the best one will be selected. It is evident that in the desired cost function, future values of system state variables exist and must be predicted by the system model in any control intervals. Although predictive control of induction machine has suitable results but the main advantage of DTC i.e. its simplicity will be omitted because of its very high computational volume compared with the DTC method.

The second stage of the proposed approach is optimizing the weighting factor of the selected fitness function by multiple simulating the control system in aspect of an optimality criterion. In the final stage of the proposed approach, the selected fitness function and its optimum weighting factor are examined in multiple operating points to extract the average boundaries of sectors that the suggested vectors would be changed and the final modified switching table of the proposed approach will be extracted. The final proposed switching table is similar to the classic DTC switching table but it has some differences and improved performance in aspect of selected optimality criterion. It is obvious that the proposed method has the same simplicity and low calculation volume compared with the classic DTC. Also with this proposed approach, other optimality aspects such as faster dynamics, higher efficiency, and so on can be applied and a new switching table can be extracted. The stages of the proposed approach have been described in the next subsections.

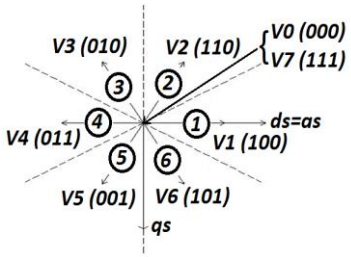

Fig. 2 The switching vectors of conventional VSI and sectors.

Table 1 The effect of different switching vectors on machine torque and flux amplitudes in sector *n*.

Vector	V_{n-2}	V_{n-1}	V_n	V_{n+1}	V_{n+2}	V_{n+3}
Flux	↓	↑	↑	↑	↓	↓
Torque	↓	↓	-	↑	↑	-

3.1 Calculation of Difference Values

At the first stage, in any time intervals of control, the predicted differences (refereed by Δ) of torque and flux amplitudes per all switching vectors are calculated. According to machine equations, the difference of machine flux amplitude can be calculated by (2)-(4).

$$\left|\Delta\lambda(k)\right| = \sqrt{\left(\lambda_{ds}+\Delta\lambda_{ds}(k)\right)^2+\left(\left(\lambda_{qs}+\Delta\lambda_{qs}(k)\right)\right)^2} - \sqrt{\lambda_{ds}{}^2+\lambda_{qs}{}^2} \tag{2}$$

$$\Delta\lambda_{ds}(k) = \left(v_{ds}(k)-R_s i_{ds}\right)\Delta t \tag{3}$$

$$\Delta\lambda_{qs}(k) = \left(v_{qs}(k)-R_s i_{qs}\right)\Delta t \tag{4}$$

where Δt is the control time interval and k = 1, 2, …, 8 is the number of inverter vectors. The voltage components for any switching vector can be reconstructed by DC link value and switching states of the inverter for any vectors according to (5) and (6), and current components will be calculated from phase currents by (7) and (8) where s_a, s_b, s_c refers to the switching states of the inverter legs.

$$V_{ds}(k) = \frac{2}{3}V_{dc}\left(s_a(k)-\frac{1}{2}s_b(k)-\frac{1}{2}s_c(k)\right) \tag{5}$$

$$V_{qs}(k) = \frac{2}{3}V_{dc}\left(\frac{\sqrt{3}}{2}s_b(k)+\frac{\sqrt{3}}{2}s_c(k)\right) \tag{6}$$

$$i_{ds} = \frac{2}{3}\left(i_a - \frac{1}{2} i_b - \frac{1}{2} i_c \right) \quad (7)$$

$$i_{qs} = \frac{2}{3}\left(\frac{\sqrt{3}}{2} i_b - \frac{\sqrt{3}}{2} i_c \right) \quad (8)$$

Also according to the induction machine equations, the electromagnetic torque and the stator currents differences can be derived as (9) and (10).

$$\begin{aligned} \Delta T(k) = \frac{3}{2} P \{ & \left[\left(\lambda_{ds} + \Delta\lambda_{ds}(k) \right) \left(i_{qs} + \Delta i_{qs}(k) \right) \right] \\ & - \left[\left(\lambda_{qs} + \Delta\lambda_{qs}(k) \right) \left(i_{ds} + \Delta i_{ds}(k) \right) \right] \\ & - \left[\left(\lambda_{ds} i_{qs} \right) - \left(\left(\lambda_{qs} I_{ds} \right) \right) \right] \} \end{aligned} \quad (9)$$

$$\begin{aligned} \Delta i_{ds}(k) = & \frac{1}{L_s L_r^{'} - L_m^2} \left(L_r^{'} V_{ds}(k) - (L_r^{'} R_s + \frac{L_m^2 R_r^{'}}{L_s}) i_{ds} \right. \\ & \left. + \frac{L_m R_r^{'}}{L_r} \lambda_{dr}^{'} + \omega_r L_m \lambda_{qr}^{'} \right) \Delta t \end{aligned} \quad (10)$$

$$\begin{aligned} \Delta i_{qs}(k) = & \frac{1}{L_s L_r^{'} - L_m^2} \left(L_r^{'} V_{qs}(k) - (L_r^{'} R_s + \frac{L_m^2 R_r^{'}}{L_q}) i_{ds} \right. \\ & \left. + \frac{L_m R_r^{'}}{L_r} \lambda_{qr}^{'} - \omega_r L_m \lambda_{dr}^{'} \right) \Delta t \end{aligned} \quad (11)$$

$$\lambda_{dr}^{'} = \frac{L_r^{'}}{L_m} \lambda_{ds} + \left(L_m - \frac{L_r^{'} L_s}{L_m} \right) i_{ds} \quad (12)$$

$$\lambda_{qr}^{'} = \frac{L_r^{'}}{L_m} \lambda_{qs} + \left(L_m - \frac{L_r^{'} L_s}{L_m} \right) i_{qs} \quad (13)$$

where L_s and L'_r are the stator and refereed rotor self inductances.

3.2 The First Stage of Optimization

The optimization target could be selected among various performance measures such as torque ripple, flux ripple, weighted torque and flux ripple, drive dynamic related to maximum change of torque and flux, efficiency, etc. In classic DTC, it seems that the drive dynamic has been selected as the target for deriving the switching table. In this study, two-stages optimization has been performed for deriving a new switching table. In the first stage, in any switching intervals, a switching vector that produces maximum normalized weighted torque and flux difference along the logical commands of hysteresis controllers has been selected. Equation (14) shows the designed fitness function of this stage.

$$\begin{aligned} F(k) = & \alpha \left(\frac{\Delta T(k)}{\max\limits_{k=1..8} \left| \left(\Delta T(k) \right) \right|} \right) \times \text{sign}(h_T) \\ & + \left(\frac{\Delta\lambda(k)}{\max\limits_{k=1..8} \left| \left(\Delta\lambda(k) \right) \right|} \right) \times \text{sign}(h_\lambda), k = 1,2,\ldots,8 \end{aligned} \quad (14)$$

In this equation, α is the weighting factor that will be optimized in stage 2, h_T is the difference of reference and measured torque, and h_λ is the difference of reference and measured flux amplitude. In stage 1, the optimum vector that minimizes the above cost function will be selected in any switching intervals from inverter possible vectors. As it can be seen from (14), torque and flux differences have been normalized by their maximum values in any switching interval to eliminate the machine variables unit dependency. It is obvious that the value of the weighting factor (α) is fixed along with any simulation.

3.3 The Second Stage of Optimization

In the second stage, optimization is carried out for various weighting coefficients and operating points and the optimum weighting factor for reduced torque ripple has been found to overcome the main drawback of classic DTC. In this stage, the fitness function is the standard deviation of the torque ripple along with the simulation for all selected operating points. Equation 15 shows the fitness function of this stage.

$$\sigma(\alpha) = \frac{\sqrt{\sum_{k=1}^{n} \left(T_e(k) - \overline{T_e} \right)^2}}{n}, \alpha = 0..200, k = 1..n \quad (15)$$

where n is the number of time samples along with simulation after transient time and *Te* is the machine electromagnetic torque. At this stage, various simulations are carried out for various weighting factors, and at the end of any simulation, the standard deviation of machine electromagnetic torque being calculated for the selected α. The same process is repeated for various operating points in the aspect of operating speed and load torque. Finally, all calculated standard deviations will be used to select the optimum weighting factor which minimizes the machine torque ripple in all operating points.

Now, the optimum weighting factor and its related standard deviation data for all operating points have been used for deriving the final fixed switching table. For this reason, all the selected optimum vectors and the related flux angles are stored in any switching intervals, and then these data are plotted in figures such as Fig. 12. The switching boundaries, intervals length and suggested vectors in any interval can be simply observed and extracted for any operating point. Now the boundaries of the resulted figures can be averaged to derive the final switching table.

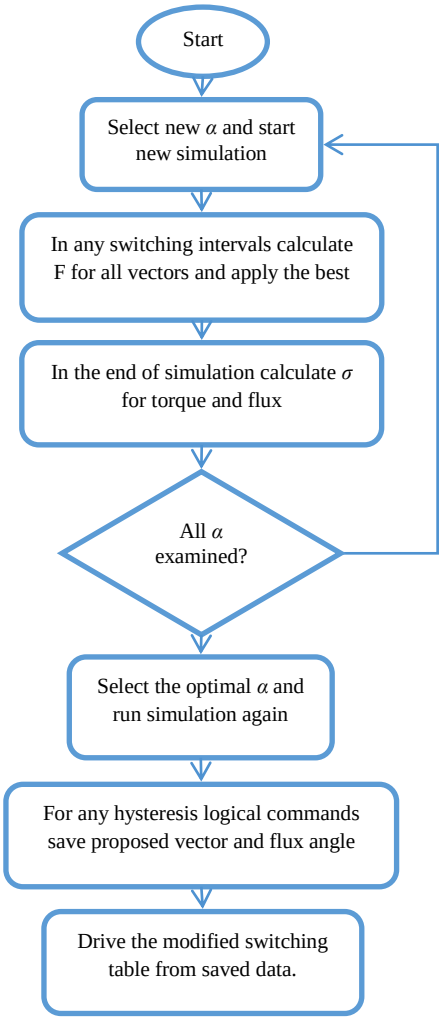

Fig. 3 The optimization flowchart in the design stage.

It is worth notable that two-stage mentioned optimizations are only for deriving a new switching table in the design stage and they would not be applied in operation mode therefore the simplicity of classic DTC will be maintained unchanged. Fig. 3 shows the optimization flowchart in the design stage.

4 Results

The mentioned two-stage optimization applied on a standard induction machine manufactured by MotoGen company with parameters listed in Table 2. The values of internal parameters have been derived by classic DC, no-load, and locked rotor experiments.

The optimization simulations have been carried out for four operating points and numerous weighting factors. Because of page limitation, only the waveforms of one operating point (ω_{ref} = 50% nominal, T_L = 75% nominal) and some weighting factors have been provided and the other results are presented in numeric forms.

4.1 Detailed Comparison of Switching Instances (Initial Concept)

At first, for initial comparing the classic DTC and proposed scheme, the amount of vector similarity called overlapping in all switching instances of two methods has been derived and depicted in Fig. 4. As it can be seen, two methods have a maximum overlapping percentage of switching vectors along the simulation time with a weighting factor 2.3 in the selected operating point.

The maximum overlapping percentage in this operating point is 91.75%. This means that in 8.25 percent of switching points, there are other vectors different from the classic DTC proposed vector that not only reply to the hysteresis commands but also can provide additional benefits such as ripple reduction and so on. These differences mostly occur when the sector of flux angle changes. For more illustration, three sample points are depicted in Table 3.

With detailed investigation of switching instances with different suggested vectors, it can be seen that the differences occur in sectors boundary. The aim of Table 3 data is to answer to challenges questioned in the introduction section and they are a simulation proof that the boundaries, sectors and suggested vectors in classic DTC can be changed and cannot be considered fixed

Table 2 Motor parameters.

Machine Type	MotoGen 80-4B
Nominal Power	750 W
Nominal Torque	5.186 N.m
Nominal Voltage	380 V
fn	50 Hz
Nominal Speed	1381 rpm
R_s	10.274 Ω
L_{ls}	0.0285 H
R'_{lr}	8.633 Ω
L'_{lr}	0.0285 H
L_m	0.37135 H
J	0.02 Ks.m^2
B	0.005752 N.m.s
Pole pairs	2

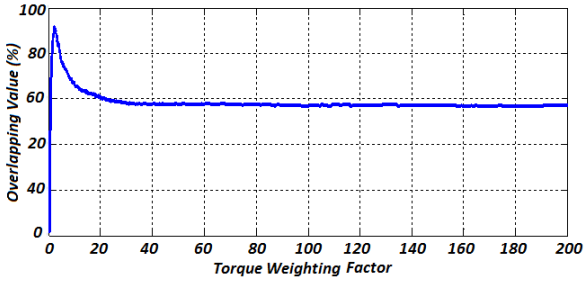

Fig. 4 The overlapping percentage of classic DTC and the proposed method in one operating point.

Table 3 Detailed comparison of three switching instances.

Time	0.3962	0.5149	0.9032
h_T	1	1	-1
h_λ	1	1	-1
Sector	6	1	3
DTC Vector	1	2	1
ΔT [N.m] with DTC vector	0.82	0.7914	-2.0101
$\Delta\lambda$ [mWeb] with DTC vector	0.417	4.43	-4.96
Fitness value for DTC vector	1.1134	0.9666	2.4406
Vector with the best fitness	6	1	6
ΔT [N.m] with best vector	0.1421	0.1876	-1.4524
$\Delta\lambda$ [mWeb] with best vector	0.0322	0.0301	-0.0353
Fitness value for best vector	1.1165	1.1117	2.6618

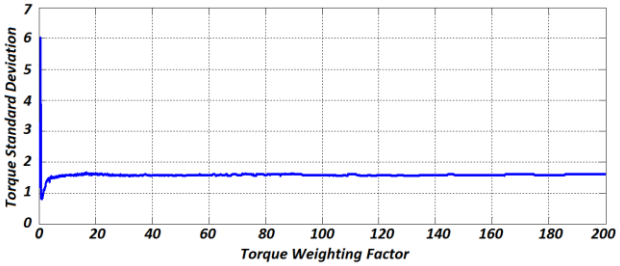

Fig. 5 Variation of torque standard deviation with respect to weighting factor.

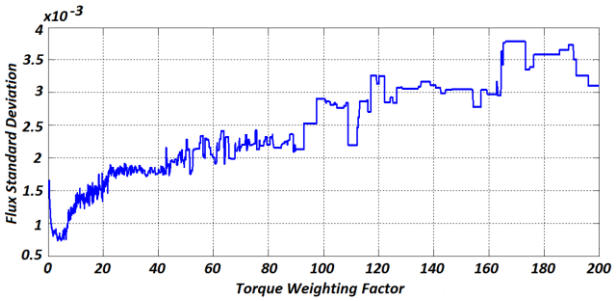

Fig. 6 Variation of flux standard deviation with respect to weighting factor.

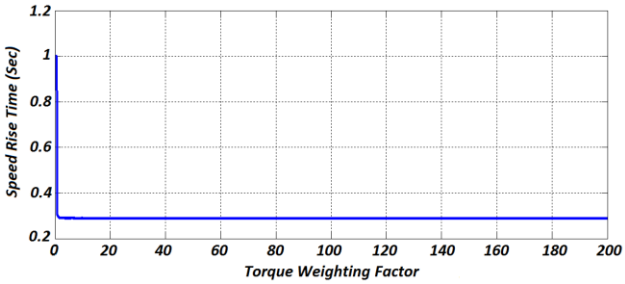

Fig. 7 Variation of speed rising time with respect to weighting factor.

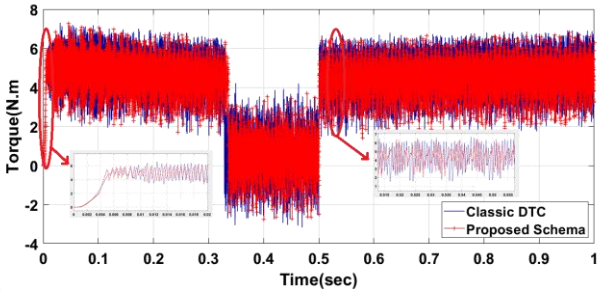

Fig. 8 Machine torque response for classic DTC and the proposed method with weighting factor 1.

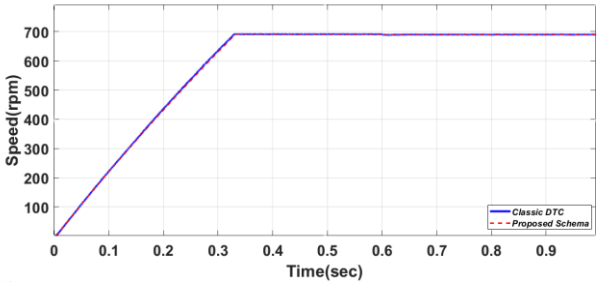

Fig. 9 Machine speed response for classic DTC and the proposed method with weighting factor 1.

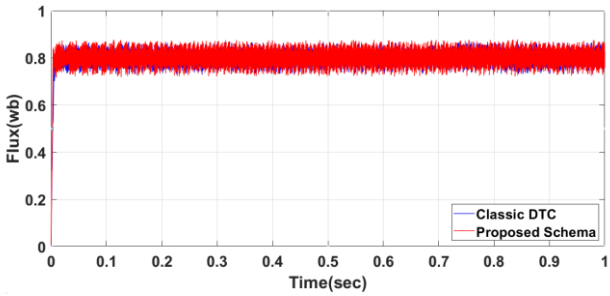

Fig. 10 Machine stator flux magnitude for classic DTC and the proposed method with weighting factor 1.

values. It can be seen that the classic DTC and selected fitness function suggest different vectors, especially in boundaries. Its means that to increase performance, the sectors with 60° intervals and crisp edges can be violated.

4.2 Optimality Aspects Discussion

Now some simulations are carried out by increasing the weighting factor of fitness function (α in (14)) and studying the variation of performance factors such as torque and flux standard deviations and speed rising time. Figs. 5-7 show the standard deviation variation of torque, flux, and speed rising time with respect to the weighting factor respectively. In these figures, the weighting factor being varied monolithically from zero to 200 and the simulations have run for any value of α. At the end of any simulation, the standard deviation of steady-state torque (Fig. 5), the standard deviation of flux (Fig. 6), and the rising time (Fig. 7) have been calculated and saved.

As can be seen from these figures, for the first operating point, the minimum standard deviation of machine torque and flux occurred approximately in weighting factors 1 and 3.9, respectively. It is also notable that σ_T and rising time vary slightly with increasing α but σ_λ varies very high, therefore high values for weighting factor is not appropriate. Figs. 8-11 show the machine torque, speed, magnitude of stator flux, and phase A current for classic DTC and proposed method for operating point with speed command 50% and load torque 100% nominal (applied on time 0.5 sec) and weighting factor 1, respectively. It is obvious that the torque ripple has been reduced with the proposed method. It is notable that probably by looking at Fig. 11, starting current of the proposed method seems is higher compared to classic DTC but it not correct because phase B current in classic DTC has the same higher stating current.

The standard deviation of machine torque, flux, and rising time of speed for selected operating point for classic DTC and proposed method with maximum overlapping weighting factor (α = 2.3) and minimum standard deviation of machine torque (α = 1) have depicted in Table 4. As it can be seen, the proposed method with a weighting factor equal to 2.3, can

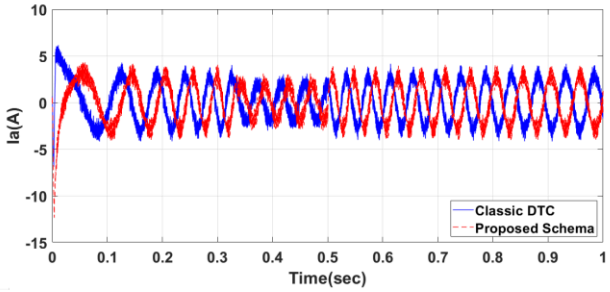

Fig. 11 Machine stator current (Phase A) for classic DTC and proposed method with weighting factor 1.

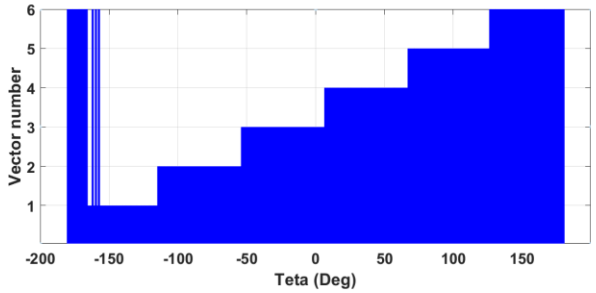

Fig. 12 Suggested vectors with proposed method (weighting factor 1 and hysteresis commands h_T = 1, h_λ = -1.

Table 4 Comparison of some performance factors for two methods.

Method	σ_T	σ_λ	t_r
Classic DTC	1.3917	8.3324×10^{-4}	0.2927
Proposed method with α = 2.3	1.2393	8.7019×10^{-4}	0.2909
Proposed method with α = 1	0.8043	10.49×10^{-4}	0.2994

Table 5 Sector boundaries with proposed method (weighting factor 1 and hysteresis commands h_T = 1, h_λ = -1).

Sector title		*A*	*B*	*C*	*D*	*E*	*F*
θ [Deg]	From	-49.81	10.83	70.63	130.75	-169.95	-109.38
	To	9.92	69.41	129.93	-171	-110.24	-49.92
Vector number		3	4	5	6	1	2

improve the standard deviation of torque and rising time 10.93% and 0.62% respectively but the standard deviation of flux deteriorated 4.24%. Also with weighting factor 1, the standard deviation of torque can be improved by 42.2% but the standard deviation of flux and rising time deteriorated by 20.5% and 6.7 ms, respectively.

It can be seen from this table, although the standard deviation of flux in classic DTC is smaller than in the proposed method with α = 1 approximately 20.5%, but the standard deviation of torque is smaller approximately 42% for the proposed method. It must be noted that the torque ripple is the primary performance factor of a drive system and it is the main drawback of the DTC method but flux ripple is a secondary parameter that is important because leads to torque ripple. Therefore reduction of torque ripple has a priority to the reduction of flux ripple and for this reason, the weighting factor 1 has been selected to drive the proposed switching table.

4.3 Sector Intervals and Boundaries

In classic DTC, switching vectors are determined every 60-degree interval (Sectors) with fixed boundaries. Some beneficial results from simulations have been extracted to challenge the validity of this issue. Fig. 12 and Table 5 show sample results for the aforementioned operating point with one state of hysteresis commands (h_T = 1, h_λ = -1) and one weighting factor. As it can be seen the boundaries and intervals length can be changed for enhanced performance with the proposed method. Similar results for other operating points, hysteresis commands, and weighting factors have been extracted and validate these results. In Table 5, because of different sectors in the proposed method compared to classic DTC, instead of sector numbers other sector titles have been used.

4.4 Final Proposed Method With Novel Switching Table

It is obvious that the proposed method till now has a high computational burden and cannot be compared with classic DTC with a simple switching table. In the proposed method for a given weighting factor, in each switching instances, the torque and flux differences for all switching vectors must be calculated and the optimum vector will be selected according to a fitness function. In this section, a new optimal switching table with different intervals boundaries and lengths will be proposed that has been derived from numerous simulations in different operating points. The final proposed method is quite similar to classic DTC but it has a modified switching table that can increase the control performance. After numerous simulations in design stage, the weighting factor 1 is suggested and the optimum switching table has been proposed in Table 6. The vectors and boundaries of the proposed switching table have been extracted by plotting the suggested vectors with respect to flux angle for various operating points. Then angles of their boundaries for the same vectors and the same torque and flux difference commands averaged. It is interesting that note, as it is proved in design stage simulations, the boundaries and length of switching interval must be varied for any states of hysteresis commands. For example the new sectors for h_T = 1 and h_λ = -1 are depicted in Fig. 13.

Table 6 Final proposed switching table.

Sector title			*A*	*B*	*C*	*D*	*E*	*F*
λ=-1 T=-1	θ [Deg]	From	-63.3	-4.10	55.16	115.91	175.21	-130.6
		To	-4.11	55.15	115.9	175.2	-130.7	-63.2
	Vector number		4	5	6	1	2	3
λ=1 T=-1	θ [Deg]	From	-47.45	10.35	70.05	130.77	-168.35	-110.21
		To	10.34	70.04	130.76	-168.36	-110.22	-47.44
	Vector number		6	1	2	3	4	5
λ=-1 T=1	θ [Deg]	From	-49.81	9.93	69.42	129.94	-171.05	-110.23
		To	9.92	69.41	129.93	-171.06	-110.24	-49.82
	Vector number		3	4	5	6	1	2
λ=1 T=1	θ [Deg]	From	-66.27	-8.30	51.35	111.97	171.85	-128.47
		To	-8.31	51.34	111.96	171.84	-128.48	-66.28
	Vector number		1	2	3	4	5	6

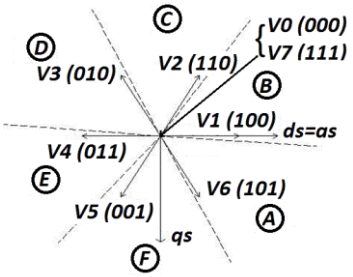

Fig. 13 New sectors for hysteresis commands $h_T = 1$, $h_\lambda = -1$.

Table 7 Comparison of DTC with classic and proposed switching tables.

Operating point	Method	t_r	σ_λ	σ_T
Torque = 75%	DTC with classic table	0.2927	8.3324×10^{-4}	1.3917
Speed = 50%	DTC with proposed table	0.2992	1×10^{-4}	0.8246
Torque = 25%	DTC with classic table	0.2927	9.31×10^{-4}	2.1497
Speed = 50%	DTC with proposed table	0.2992	0.0011	1.3437
Torque = 50%	DTC with classic table	0.4631	8.28×10^{-4}	2.0788
Speed = 75%	DTC with proposed table	0.4669	9.76×10^{-4}	1.39
Torque = 50%	DTC with classic table	0.1412	9.23×10^{-4}	2.0754
Speed = 25%	DTC with proposed table	0.1437	9.93×10^{-4}	1.3047

It must be noted that the structure of the proposed DTC does not differ from classic DTC and its structure is the same as Fig. 1. The only difference is its switching table that is proposed in Table 6.

For verification of proposed switching fixed table and comparison of results with classic DTC in aspect of optimality factors, two methods have simulated in various operating points and results have depicted in Table 7. It is obvious that the proposed method decreases the torque deviation significantly in all operating points but the flux deviation and speed rising time deteriorate very slightly. Therefore the proposed method does not also have any additional computational burdens but also has better performance factors compared with classic DTC.

5 Conclusion

In this paper, a conceptual study on switching intervals in the classic direct torque control (DTC) method has been challenged in aspects of length and boundaries of switching intervals, optimality target of switching table, and operating point effect on them. It is proved by simulations that all these issues can be altered. Finally, a new switching table with different lengths and boundaries of intervals has been proposed that could improve the DTC performance in aspect of its main drawback i.e. torque ripple. It is worth notable, although the proposed final switching table has been derived by a two-stage optimization process with high computational efforts but these computations would be done once in the design stage. Therefore the proposed method not also has the main advantage of the DTC method i.e. its simple implementation but also it has a lower degree of classic DTC main drawback i.e. torque ripple.

References

[1] N. P. Quang and J. A. Dittrich, *Vector control of three-phase AC machines*. Heidelberg: Springer, 2015.

[2] P. Vas, *Sensorless vector and direct torque control*. Oxford Univ. Press, 1998.

[3] F. Blaschke, "A new method for the structural decoupling of AC induction machines," in *Conf. Rec. IFAC*, Dusseldorf, Germany, pp. 1–15, 1971.

[4] I. Takahashi and T. Noguchi, "A new quick-response and high-efficiency control strategy of an induction motor," *IEEE Transactions on Industry Applications*, Vol. IA-22, No. 5, pp. 820–827, 1986.

[5] M. Nemec and D. Nedeljkovi, "Predictive torque control of induction machines using immediate flux control," *IEEE Transactions on Industrial Electronics*, Vol. 54, No. 4, pp. 2009–2017, 2007.

[6] Zh. Zhang, R Tang, B. Bai, and D. Xie, "Novel direct torque control based on space vector modulation with adaptive stator flux observer for induction motors," *IEEE Transactions on Magnetics*, Vol. 46, No. 8, pp. 3133–3136, 2010.

[7] Y. Zhang and J. Zhu, "A novel duty cycle control strategy to reduce both torque and flux ripples for DTC of permanent magnet synchronous motor drives with switching frequency reduction," *IEEE Transactions on Power Electronics*, Vol. 26, No. 10, pp.3055–3067, 2011.

[8] M. Bertoluzzo, G. Buja, and R. Menis, "Direct torque control of an induction motor using a single current sensor," *IEEE Transactions on Industrial Electronics*, Vol. 53, No. 3, pp. 778–784, 2006.

[9] B. Metidji, N. Taib, L. Baghli, T. Rekioua, and S. Bacha, "Low-cost direct torque control algorithm for induction motor without AC phase current sensors," *IEEE Transactions on Industrial Electronics*, Vol. 27, No. 9, pp. 4132–4139, 2012.

[10] P. C. Krause, O. Wasynczuk, and S. D. Sudhoff, *Analysis of electric machinery and drive system*. New York: IEEE Press, 2002.

[11] W. Wang, M. Cheng, W. Hua, S. Ding, Y. Zhu, and W. Zhao, "Low-cost SVM-DTC strategy of induction machine drives using single DC-link current sensor," *Journal of International Conference on Electrical Machines and Systems*, Vol. 1, No. 3, pp. 266–273, 2012.

[12] M. Vasudevan, R. Arumugam, and S. Paramasivam, "Development of torque and flux ripple minimization algorithm for direct torque control of induction motor drive," *Electrical Engineering*, Vol. 89, No. 1, pp. 41–51, 2006.

[13] J. Beerten, J. Verveckken, and J. Driesen, "Predictive torque control for flux and torque ripple reduction," *IEEE Transactions on Industrial Electronics*, Vol. 57, No. 1, pp. 404–412, 2010.

[14] M. Ouhrouche, R. Errouissi, A. M. Trzynadlowski, K. A. Tehrani, and A. Benzaioua, "A novel predictive direct torque controller for induction motor drives", *IEEE Transactions on Industrial Electronics*, Vol. 63, No. 8, pp. 5221–5230, 2016.

[15] M. Habibullah, D. D. C. Lu, D. Xiao, and M. F. Rahman, "A simplified finite-state predictive direct torque control for induction motor drive," *IEEE Transactions on Industrial Electronics*, Vol. 63, No. 6, pp. 3964–3975, 2016.

[16] F. Wang, S. A. Davari, D. A. Khaburi, and. R. Kenel, "Sensorless model predictive torque control for induction machine by using the sliding mode full-order observer," in *IEEE Symposium on Sensorless Control for Electrical Drives (SLED)*, Birmingham, pp. 114–117, 2011.

A. Ghayebloo received the B.Sc. degree from the Sahand University of Technology in 2004, M.Sc. degree from Amirkabir University of Technology (Tehran Polytechnic) in 2007, and Ph.D. degree from KNT University of Technology at 2013 all in Electrical Engineering. He has joined to Engineering Department of University of Zanjan as academic staff since 2013. Dr. Ghayebloo also is the Director of D&M research laboratory. His research interests address all aspects of power electronics, electrical machines, and drives, hybrid vehicles, and instrumentation.

S. Shiri received the B.Sc. degree from Technical and Vocational University, Zanjan Alghadir school in 2017, and M.Sc. degree from the University of Zanjan in 2019 all in Power Engineering. His research interests are electric machines drives and power electronics.